Comprehensive Design Approach for Field-Oriented Control of Interior Permanent Magnet Synchronous Machines

Comprehensive Design Approach for Field-Oriented Control of Interior Permanent Magnet Synchronous Machines

Tiago Davi Curi Busarello, *Senior Member, IEEE*
Department of Control, Automation and Computation Engineering
Federal University of Santa Catarina
Blumenau, Brazil
tiago.busarello@ufsc.br

Abdullah Bubshait
Deptartment of Electrical Engineering
King Faisal University
Alahsa, Saudi Arabia
asbubshait@kfu.edu.sa

Oruganti V.S.R.Varaprasad, *Member, IEEE*
Department of Electrical and Electronics Engineering
Gayatri Vidya Parishad College of Engineering (Autonomous)
Visakhapatnam, Andhra Pradesh, India
varaprasad.oruganti@ieee.org

Abdulhakeem Alsaleem
Department of of Electrical Engineering
Qassim University
Buraydah, Saudi Arabia
eng.hakeem@qec.edu.sa

Marcelo G. Simões, *Fellow, IEEE*
School of Technology and Innovations
University of Vaasa
Vaasa, Finland
marcelo.godoy.simoes@uwasa.fi

***Abstract*—This paper presents a comprehensive design approach for a field-oriented control of Interior Permanent Magnet Synchronous Machines (IPMSM). Initially, the IPMSM model is revisited. Later, a step-by-step procedure for designing a Field Oriented Control (FOC) Strategy for IPMSM is presented. The control strategy is in *dq*-rotating reference frame and it is synchronized with the rotor position. The current controllers are designed based on setting a desired closed-loop time-constant while the speed controller is designed based on a frequency response approach, which is different from the conventional methods. The proposed approach supplies all the steps to accurately tuning the parameters of the Proportional-Integrator (PI) controllers of the current and speed control loops. Furthermore, the proposed design approach is a fast, reliable and accurate guide to implement IPMSM drive based on FOC. Results from a Hardware-in-Loop (HIL) with external microcontroller are presented. The comprehensive design approach is verified under two different IPMSM parameters and the results showed its effectiveness.**

***Index Terms*—Electric machines, hardware-in-the-loop simulation, machine vector control, permanent magnet machines, Variable speed drives.**

I. Introduction

Permanent Magnetic Synchronous Machine (PMSM) Drive is a mature technology and widely used in the engineering field. In recent yeas, PMSMs gained considerable attention due to its application in the Electric Vehicle area mainly because of their high-power density, low maintenance and high controllability. PMSMs are usually built with surface or interior magnets, being the last more favorable for high-speed applications. For such a case, the machine is called Interior Permanent Magnet Synchronous Machine (IPMSM). A feature of these machines is that the quadrature and direct inductance have equal values for surface-mounted machines while they have different values for interior-mounted ones [1].

Two of the most common control strategies for IPMSMs are the Field Oriented Control (FOC) and Direct Torque Control (DTC). The FOC principle is to control the stator current in a reference frame as well as the IPMSM speed. The reference frame can be the stator flux, rotor flux, among others. By measuring the IPMSM stator current and transforming the measured variable from *abc* to *dq* using the rotor flux reference frame, the *d*-axis and *q*-axis can be controlled separately. In this case, the i_q is called torque-producing current while the i_d is called flux-producing current. Regarding the speed control, its output signal is used as reference for the *q*-axis. The reference for *d*-axis is usually set as zero to minimize the reluctant torque.

Still regarding the FOC strategy, the rotor position must be obtained either by a resolver or by observers [2]–[4]. The *dq*-axis current control and the speed control are usually done by Proportional-Integral (PI) controllers [5]. Therefore, the FOC strategies uses three PI controllers. It deserves attention the fact that the *dq*-axis are coupled in the FOC strategy.

Books and papers available in the literature covers the pro-

The authors thank to *Fundação de Amparo à Pesquisa e Inovação do Estado de Santa Catarina - FAPESC*, Brazil, for supporting this research under the grant 2021TR000306

cedures for tuning the PI controllers of a FOC for PMSM [6]–[13]. Most of them describe the procedure considering surface-mounted and interior magnets machines in a unique approach. Regarding these papers, the majority of them employs FOC in PMSM applications, but the approach for tuning the PIs do not gain the deserved attention, mainly because the focus of the papers is on another topic. Specially for the speed controller, its tuning procedure is usually not described in a frequency response approach, which is an attractive and accurate tool.

In this context, a comprehensive design approach for FOC strategy of IPMSM is needed. The proposal design approach of this paper describes the step-by-step procedure for tuning the PIs of a IPMSM drive based on FOC strategy as well as present details for a proper performance of the IPMSM drive. To verify the efficacy of the proposal design approach, the system is tested in a Hardware-in-Loop (HIL) device with an external microcontroller. In other words, the IPMSM and the inverter run within the HIL 402 from Typhoon company while the whole control strategy runs in the TMS320F28335 microcontroller.

II. System Description

Fig. 1 presents the system perspective. The system has a DC-source, which may come from a front-end rectifier, a three-phase inverter and the IPMSM. The phases A, B and C of the stator current (i_a, i_b, i_c) are measured and sent to the control strategy block. The measurement of stator current for phase C could be eliminated and its value could be computed within the microcontroller. Similarly, the machine electrical speed (ω) and the electric rotor angle (θ) are also obtained using position and speed transducers, even though this could be estimated with observers.

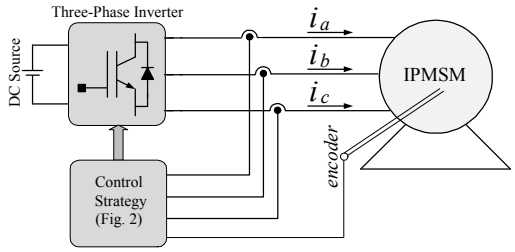

Fig. 1. The system perspective.

Fig. 2 presents the control strategy block diagram of FOC. The three-phase stator current is converted to dq-rotating reference frame. The d-axis current is compared with zero and the resulting signal is sent to the PI controller (PI_d). For q-axis current, the comparison is with the output signal of the the PI controller of the speed mesh (PI_s). Then, the resulting signal is sent to the PI controller (PI_q) of the q-axis. The PI controllers will be later called as $G_{iq}(s)$ and $G_{id}(s)$. After the PI of the dq-axis, there is the decoupling scheme and the inverter gain compensation. At the end, the dq-axis signals are converted back to abc-reference frame and its output is modulated using Space Vector Pulse-Width Modulator (SVPWM). L_d and L_q are the direct- and quadrature-axis inductance, respectively. λ is the flux linkage of the rotor magnets. Vdc is the value in Volts of the DC source showed in Fig. 1.

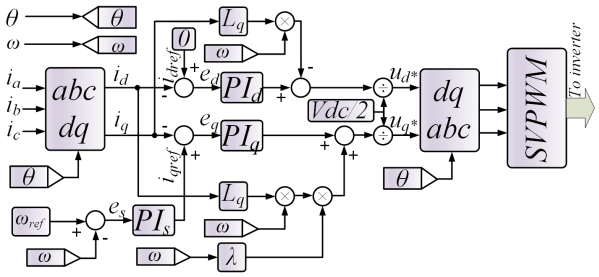

Fig. 2. Control Strategy Block Diagram of FOC.

III. Dynamic Model for IPMSM

Before presenting the step-by-step procedure of tuning the PIs for the FOC strategy, it is convenient to present the equations that describe the dynamic behavior of the IPMSM. The equations are in rotor-reference frame. Some assumptions for IPMSM modeling are: the stator windings of the machine are distributed sinusoidally; sinusoidal flux density around the machine air gap; the machine is supplied by a converter system with no switching harmonics; core and stray losses are ignored and the machine has sinusoidal induced EMF.

A. Dynamic Electric Model for IPMSM

The IPMSM dynamic behavior is described by the following equations:

$$v_{qs} = R_s i_{qs} + L_q \frac{di_{qs}}{dt} + \omega_r L_d i_{ds} + \omega_r \lambda_{af} \tag{1}$$

$$v_{ds} = R_s i_{ds} + L_d \frac{di_{qs}}{dt} - \omega_r L_d i_{ds} \tag{2}$$

where v_{qs} and v_{ds} are the stator voltage for q and d axis, i_{qs} and i_{ds} are the stator current for q and d axis, L_q and L_d are the inductance for q and d axis, ω_r is the electrical speed and ω_{af} is the air gap flux linkage.

Defining two new variables as:

$$u_q = -\omega_r L_d i_{ds} - \omega_r \lambda_{af} + v_{qs} \tag{3}$$

$$u_d = \omega_r L_d i_{ds} + v_{ds} \tag{4}$$

Therefore, (1) and (2) can be written as the following equations. They are in accordance to the decoupling scheme of Fig. 2.

$$u_q = R_s i_{qs} + L_q \frac{di_{qs}}{dt} \tag{5}$$

$$u_d = R_s i_{ds} + L_d \frac{di_{qs}}{dt} \tag{6}$$

As a result of that, the previous equations represent two decoupled subsystems and two independent controllers can be employed to make the i_d and i_q follow their reference signals. Taking the Laplace transformation of (5) and (6) and arranging

them, one can get (7) and (8). These equations are the system's plant for the current control meshes.

$$G_{id}(s) = \frac{K_s}{1 + s\tau_d} \tag{7}$$

$$G_{iq}(s) = \frac{K_s}{1 + s\tau_q} \tag{8}$$

where,

$$K_s = 1/R_s; \tau_d = \frac{L_d}{R_s}; \tau_q = \frac{L_q}{R_s} \tag{9}$$

The abc to dq conversion is obtained through two parts using (10) and (11). For dq to abc their inverted matrixes are used.

$$\begin{bmatrix} i_\alpha \\ i_\beta \end{bmatrix} = \begin{bmatrix} \frac{2}{3} & \frac{-1}{3} & \frac{-1}{3} \\ 0 & \frac{1}{\sqrt{3}} & \frac{-1}{\sqrt{3}} \end{bmatrix} \begin{bmatrix} i_a \\ i_b \\ i_c \end{bmatrix} \tag{10}$$

$$\begin{bmatrix} i_d \\ i_q \end{bmatrix} = \begin{bmatrix} sin(\theta) & -cos(\theta) \\ cos(\theta) & sin(\theta) \end{bmatrix} \begin{bmatrix} i_\alpha \\ i_\beta \end{bmatrix} \tag{11}$$

B. Dynamic Mechanical Model for IPMSM

The electromechanical torque is given by:

$$T_e = \frac{3}{2}\frac{P}{2}\lambda_{af} i_{qs} + (L_d - Lq) i_{ds} i_{qs} \tag{12}$$

where P is the number of poles. For i_{ds}, (12) results in:

$$T_e = \frac{3}{2}\frac{P}{2}\lambda_{af} i_{qs} \tag{13}$$

The electrical torque can also be written as:

$$T_e = K_{te} i_{qs} \tag{14}$$

where

$$K_{te} = \frac{3}{4} P \lambda_{af} \tag{15}$$

IV. Step-by-Step Procedure

The step-by-step procedure for designing the PIs of the FOC strategy is divided into two parts: one for the current controller and another one for speed controller, as follow.

A. Current Controller

According to Section III.A, the PIs of the current control mesh can be designed using the simplified block diagram shown in Fig. 3.

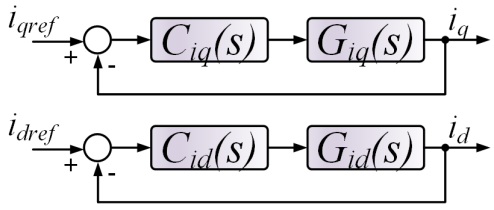

Fig. 3. Simplified Control Strategy Block Diagram for Designing the Current Controllers.

The C_{iq} and C_{id} are the PI controllers and given respectively by:

$$C_{iq}(s) = \frac{k_{pq}s + k_{iq}}{s} \tag{16}$$

$$C_{id}(s) = \frac{k_{pd}s + k_{id}}{s} \tag{17}$$

1st step: knowing the system parameters: The first step in designing the FOC strategy for IPMSM is to know the system parameters. Tab. I shows the parameters and their unit that must be known.

TABLE I
Parameters and their Units

Parameters	Unit
Stator Resistance (R_s)	Ω
Direct inductance (L_q)	H
Quadrature inductance (L_q)	H
Number of Poles (P)	$-$
Flux linkage (λ)	Wb
Moment of inertia (J)	$k_g m^2$
Rotating damper (B)	$Nm/(rad/s)$
Inverter switching frequency (f_{sw})	Hz

2nd step: defining the desired time constant for the current controllers: The second step is to define the desired closed-loop time constant for the current controllers. Such a time constant is defined as τ and its unis is seconds. τ should be small for a fast response but large enough because $1/\tau$ is the bandwidth of the closed-loop system. However, $1/\tau$ must be at least 10 times lower than switching frequency (in rad/s) of the inverter. The time constant is usually chosen in the range of 0.5 ms to 2 ms. The time constants for the dq-axis are given as;

$$\tau = \tau_{iq} = \tau_{id} \tag{18}$$

3rd step: computing the proportional gain of the q-axis PI controller: The proportional gain of the q-axis PI controller is given by:

$$k_{pq} = \frac{L_q}{\tau_{iq}} \tag{19}$$

4th step: computing the integral gain of the q-axis PI controller: The integral gain of the q-axis PI controller is given by:

$$k_{iq} = \frac{R_s}{\tau_{iq}} \tag{20}$$

By using these values for kp and Ki, a pole-zero cancellation happens and the open loop transfer function will be a simple integrator that has a gain of zero dB at the cutoff frequency that corresponds to the chosen time constant.

5th step: computing the proportional gain of the d-axis PI controller: The proportional gain of the d-axis PI controller is given by:

$$k_{pd} = \frac{L_d}{\tau_{id}} \tag{21}$$

6th step: computing the integral gain of the d-axis PI controller: The integral gain of the d-axis PI controller is given by (22). Notice tha this gain is the same for the q-axis.

$$k_{id} = \frac{R_s}{\tau_{id}} \tag{22}$$

To define the time constant of the PIs for the q- and d-axis, one may compute $\frac{k_{pq}}{k_{iq}}$ and $\frac{k_{pd}}{k_{id}}$, respectively.

B. Speed Controller

Fig. 4 presents the control strategy block diagram for designing the speed controller. The $I(s)$ is the internal current control closed loop $\frac{i_q(s)}{I_{qref}(s)}$ and can be considered as unitary since the time constant of the speed control mesh is at least ten times larger than that for the current control mesh.

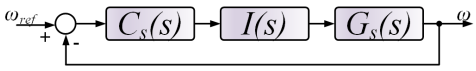

Fig. 4. Control Strategy Block Diagram for Designing the Speed Controller.

The speed controller $C_s(s)$ is given by:

$$C_s(s) = \frac{k_{ps}s + k_{is}}{s} \tag{23}$$

The speed system plant G_s is given by:

$$G_s(s) = \frac{K_a}{1 + s\frac{J}{B}} \tag{24}$$

where K_a is given by:

$$K_a = \frac{0.75P\lambda}{B} \tag{25}$$

1st step: defining the desired time constant for the speed controller: The first step in designing the speed controller is to define the desired time constant. In order to make the inter and outer loop decoupled and the inner loop as unitary, the time constant for the speed controller must be at least time times higher than the time constant of the current control mesh. Therefore, the time constant is defined in this paper as:

$$\tau_s = 10\tau_{iq} \tag{26}$$

2nd step: defining the curt-off frequency (f_c) of the closed-loop speed controller: The second step is to define a cut-off frequency for the closed-loop speed control. The choice of the cut-off frequency must be ten times lower than $1/\tau$, in Hz.

3rd step: computing the proportional gain of the speed controller: The proportional gain of the speed controller is computed through the open-loop frequency response of the speed system plant. By plotting such a frequency response and with a well defined cut-off frequency, one may pick how much is the gain a the desired cut-off frequency. Fig. 5 presents an example of how to compute the gain supposing in which the desired cut-off frequency is $200\,Hz$. G_{dB} is the gain at the desired cut-off frequency.

The proportional gain of the speed controller is then given by (27). Note that the absolute value of G_{dB} is used in the equation.

$$k_{ps} = 10^{\frac{|G_{dB}|}{20}} \tag{27}$$

4th step: computing the integral gain of the speed controller: The fourth step, the last one, is computing the integral gain of the speed controller. It is given by:

$$k_{is} = \frac{K_{ps}}{\tau_s} \tag{28}$$

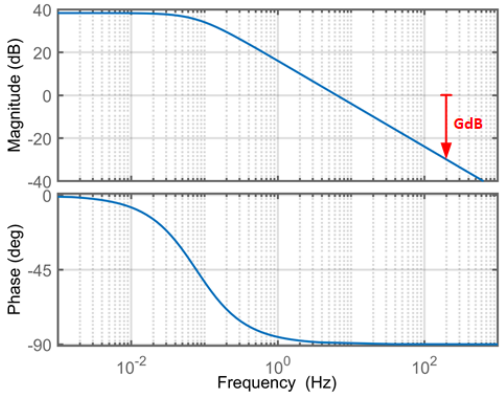

Fig. 5. An example of how to compute the gain supposing that the desired cut-off frequency is $200\,Hz$.

V. Case Studies with HIL Results

Two case studies were conducted in order to verify the proposed comprehensive design approach of FOC for IPMSM. Both of them were tested on HIL with external microcontroller. The HIL is the Typhoon HIL402 while the microcontroller is the Texas Instruments TMS320F28335. The IPMSM, the inverter and sensors run on HIL402. The FOC strategy showed in Fig. 2 runs whiting the microcontroller. In Appendix, there are a simulation results showing the controlled variables following their reference signals.

A. First case

Tab. II shows the parameter of the first case evaluated on HIL and microcontroller. The desired parameters are $\tau = 0.5\,ms$ and $f_c = 200\,Hz$. After following the step-by-step procedure for current and speed controllers, the FOC is fully designed. Tab. II also presents the designed parameters. For digital implementation of the FOC strategy into the microcontroller, the Backward Euler method was used to discretize the PI controllers.

TABLE II
System Parameter for Case 1

Parameters	Value	Parameters	Value
R_s	$1.3\,\Omega$	V_{dc}	$500\,V$
L_q	$17.2\,mH$	k_{pq}	34.39999
L_q	$8.9\,mH$	k_{iq}	2600
P	6	k_{pd}	17.8000
λ	$0.1819\,Wb$	k_{id}	2600
J	$0.0206\,k_g m^2$	k_{ps}	7.906283
B	0.01	k_{is}	59.756796
f_{sw}	$10\,kHz$		

Fig. 6 presents the electrical speed (ω), the stator current for phases a and b (i_a, i_b) and the electrical rotor position (θ) for steady-state operation. In this case, the reference speed is 2000 RPM and the load torque is 10 Nm.

Fig. 7 presents the electrical speed (ω), the stator current for phases a and b (i_a, i_b) and the mechanical load torque (T_L) for a transition of the load torque from $10\,Nm$ to $2.5\,Nm$. A zoom at the steady-state region is also presented. The electrical

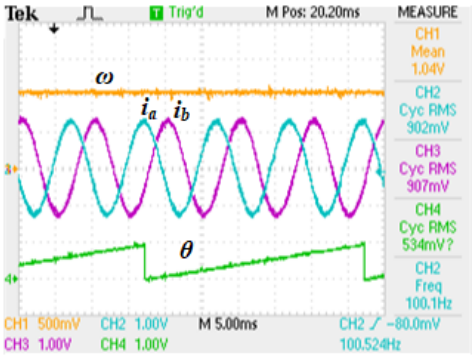

Fig. 6. The electrical speed (ω), the stator current for phases a and b (i_a, i_b) and the electrical rotor position (θ) for steady-state operation. Ch1:2000RPM/V Ch2:Ch3: 10A/V; Ch4: 20 units/V.

speed oscillates and returns to its nominal value after some seconds, indicating that speed controller as well as the current controllers are well designed.

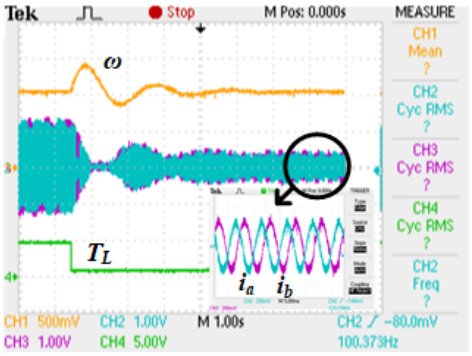

Fig. 7. The electrical speed (ω), the stator current for phases a and b (i_a, i_b) and the mechanical load torque (T_L) for a transition of the load torque from $10\,Nm$ to $2.5\,Nm$. Ch1:2000RPM/V Ch2:Ch3: 10A/V; Ch4: 2 Nm/V.

Fig. 8 presents the electrical speed (ω), the stator current for phases a and b (i_a, i_b) and the mechanical load torque (T_L) for a transition at the speed reference from $2000\,RPM$ to $1000\,RPM$. For this case, the load torque is kept constant at $10\,Nm$. A zoom in steady-state is also presented. This result shows also that the machine is correctly controlled also at $1000\,RPM$.

B. Second case

Tab. III shows the parameter of the second case evaluated on HIL and microcontroller [1]. The desired parameters are $\tau = 0.5\,ms$ and $f_c = 50\,Hz$. The designed parameters are also presented in this table.

Fig. 9 presents the electrical speed (ω), the stator current for phases a and b (i_a, i_b) and the electrical rotor position (θ) for steady-state operation. In this case, the reference speed is 2000 RPM and the load torque is 2 Nm.

Fig. 10 presents the electrical speed (ω), the stator current for phases a and b (i_a, i_b) and the mechanical load torque (T_L) for a transition of the load torque from $10\,Nm$ to $2.5\,Nm$. A zoom at the steady-state region is also presented. The electrical

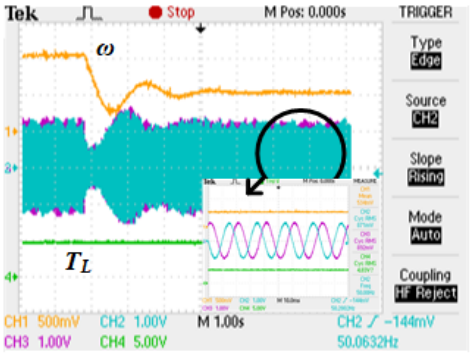

Fig. 8. The electrical speed (ω), the stator current for phases a and b (i_a, i_b) and the mechanical load torque (T_L) for a transition at the speed reference from $2000\,RPM$ to $1000\,RPM$. Ch1:2000RPM/V Ch2:Ch3: 10A/V; Ch4: 2 Nm/V.

TABLE III
SYSTEM PARAMETER FOR CASE 2

Parameters	Value	Parameters	Value
R_s	$1.2\,\Omega$	V_{dc}	$500\,V$
L_q	$12\,mH$	k_{pq}	24
L_q	$5.7\,mH$	k_{iq}	2400
P	4	k_{pd}	11.4
λ	$0.123\,Wb$	k_{id}	2400
J	$0.0005\,k_g m^2$	k_{ps}	2.349126
B	0.0001	k_{is}	23.491264
f_{sw}	$10\,kHz$		

speed oscillates and returns to its nominal value after some seconds, indicating that speed controller as well as the current controllers are well designed.

Fig. 11 presents the electrical speed (ω), the stator current for phases a and b (i_a, i_b) and the mechanical load torque (T_L) for a transition at the speed reference from $2000\,RPM$ to $1000\,RPM$. For this case, the load torque is kept constant at $2\,Nm$. A zoom in steady-state is also presented. This result shows also that the machine is correctly controlled also at $1000\,RPM$.

Fig. 12 presents a picture of the HIL setup as well as its block diagram.

VI. CONCLUSIONS

This paper proposed a comprehensive design approach for a field-oriented control of Interior Permanent Magnet Synchronous Machines. The Field-Oriented Control strategy was used in the proposed approach. The IPMSM electrical and mechanical models were first introduced. Then, a detailed step-by-step procedure for tuning the current and speed controller of FOC strategy were presented. The speed controller was designed using frequency response method. With such a procedure, two case studies with different machines were performed. The whole system was tested in a Hardware-in-Loop device with external controller. Results demonstrated the efficacy of the proposed design approach under steady-state and under steps in the reference speed and mechanical load torque. The simulation files used in this research will be freely available on the author's webpage https://busarello.prof.ufsc.br.

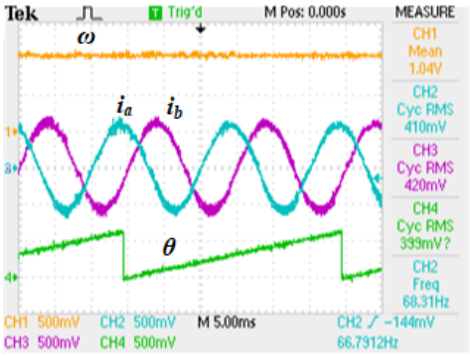

Fig. 9. The electrical speed (ω), the stator current for phases a and b (i_a, i_b) and the electrical rotor position (θ) for steady-state operation. Ch1:2000RPM/V Ch2:Ch3: 10A/V; Ch4: 20 units/V.

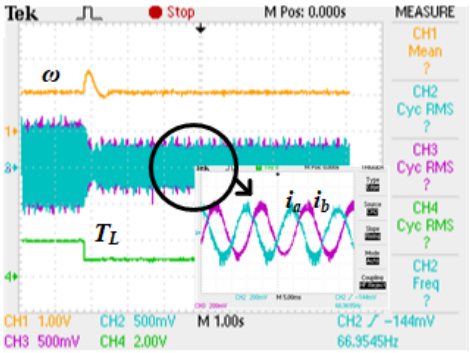

Fig. 10. The electrical speed (ω), the stator current for phases a and b (i_a, i_b) and the mechanical load torque (T_L) for a transition of the load torque from $2\,Nm$ to $1\,Nm$. Ch1:2000RPM/V Ch2:Ch3: 10A/V; Ch4: 2 Nm/V.

VII. Appendix

This Appendix presents the behavior of the controlled variables following their reference signals. Fig. 13a present dq-axis currents and their reference signals while Fig. 13b presents the IPMSM angular speed and its reference signal. The IPMSM initializes and its speed increases until reaches its set-point, given by the $wref$ line.

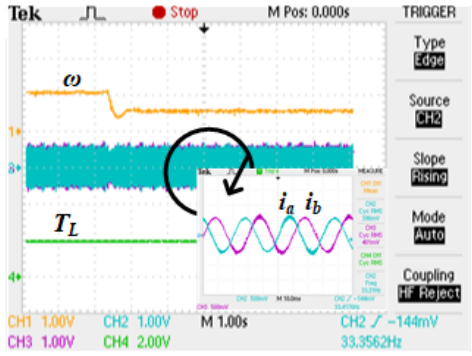

Fig. 11. The electrical speed (ω), the stator current for phases a and b (i_a, i_b) and the mechanical load torque (T_L) for a transition at the speed reference from 2000 RPM to 1000 RPM. Ch1:2000RPM/V Ch2:Ch3: 10A/V; Ch4: 2 Nm/V.

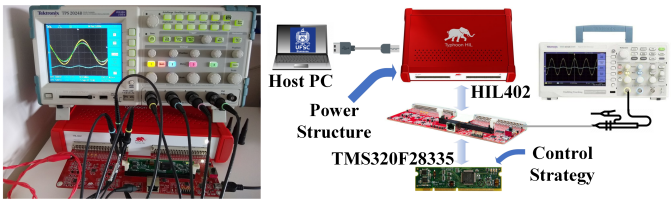

Fig. 12. A picture of the HIL setup as well as its block diagram.

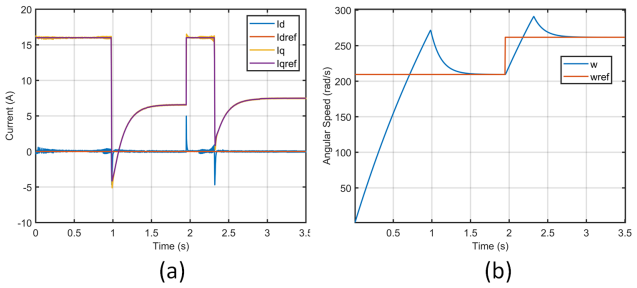

Fig. 13. (a) dq-axis currents and their reference signals and (b) The IPMSM angular speed and its reference signal.

References

[1] R. Krishnan, *Permanent Magnet Synchronous and Brushless DC Motor Drives*. CRC Press, Dec. 2017.

[2] "An Enhanced SMO-Based Permanent-Magnet Synchronous Machine (PMSM) Sensorless Drive Scheme with Current Measurement Error Compensation."

[3] "IPMSM Sensorless Control for Zero-and Low-Speed Regions under Low Switching Frequency Condition Based on Fundamental Model."

[4] "Observers for High-Speed Sensorless PMSM Drives: Design Methods, Tuning Challenges and Future Trends," vol. 9.

[5] A. Kiyoumarsi and R. Hanitsch, *Interior Permanent-magnet Synchronous Motors: Optimal Shape Design, Construction and Testing*. LAP, 2011.

[6] "A Novel SVPWM Scheme for Field-Oriented Vector-Controlled PMSM Drive System Fed by Cascaded H-Bridge Inverter," vol. 36.

[7] M. Abassi, A. Khlaief, O. Saadaoui, A. Chaari, and M. Boussak, "Performance analysis of FOC and DTC for PMSM drives using SVPWM technique," in *2015 16th International Conference on Sciences and Techniques of Automatic Control and Computer Engineering (STA)*, Dec. 2015, pp. 228–233.

[8] "PMSM Parameter Estimation for Sensorless FOC Based on Differential Power Factor."

[9] F. Hilpert, C. Bentheimer, T. Mueller, and B. Eckardt, "Investigation of Novel Multi-Phase Field-Oriented Drive Inverter Control with Fail-Operational Capabilities for Aircraft Applications," in *PCIM Europe digital days 2021; International Exhibition and Conference for Power Electronics, Intelligent Motion, Renewable Energy and Energy Management*, May 2021, pp. 1–7.

[10] A. Oprea and D. Floricau, "Field Oriented Control of Permanent Magnet Synchronous Motor with Graphical User Interface," in *2021 12th International Symposium on Advanced Topics in Electrical Engineering (ATEE)*, Mar. 2021.

[11] "Post-Fault Demagnetization of a PMSG Under Field Oriented Control Operation," vol. 9.

[12] "Field-Oriented Control and Direct Torque Control for Paralleled VSIs Fed PMSM Drives With Variable Switching Frequencies," vol. 31.

[13] C. Zhang, X. Wang, D. Wang, Q. Sun, and G. Ma, "Comparative Analysis of Electromagnetic Force Inverter Fed PMSM Drive Using Field Oriented Control (FOC) and Direct Torque Control (DTC)," in *2019 22nd International Conference on Electrical Machines and Systems (ICEMS)*, Aug. 2019.